

Fugacity-based PBTK Model of Lipophilic Contaminant Fate into Beef Cattle: Deciphering the Contaminant Properties × Lipid Nutrition × Growth Physiology Interplay

Sylvain Lerch¹, John Albechaalany¹⁻³, Charlotte Driesen^{1,2}, Philippe Schmidely³, Isabelle Ortigues-Marty⁴, Markus Zennegg², Christelle Loncke³

¹ Ruminant Research Group, Agroscope, 1725 Posieux, Switzerland, sylvain.lerch@agroscope.admin.ch

² Laboratory for Advanced Analytical Technologies, Empa, Überlandstrasse 129, 8600 Dübendorf, Switzerland

³ Université Paris-Saclay, INRAE, AgroParisTech, UMR Systemic Modelling Applied to Ruminants, 75005, Paris, France

⁴ INRAE, Université Clermont Auvergne, Vetagro Sup, UMRH, 63122 Saint-Genès-Champagnelle, France

1 Introduction

Livestock occasionally face contamination incidents with lipophilic contaminants (e.g., PCBs, PCDD/Fs), breaking down the agro-food chain, and inducing social distress for farmers¹. Bovine meat has been found to be sensitive to such contamination risks². Indeed, two monitoring studies highlighted that more than 50% of the bovine meat samples from extensive farming systems exceeded either the action (product sale permitted, contamination source should be identified) or maximum (product sale prohibited, confiscation and incineration) regulatory levels^{3,4}. Understanding the fate of lipophilic contaminants in beef cattle is the cornerstone for a fair risk assessment. It is classically investigated via feeding experiments, from which feed-to-meat bioconcentration and biotransfer factors are computed. In such an approach, the animal system is seen as a ‘black box’ and the transfer factor is given as a single average value. Nonetheless, the rate of feed-to-meat transfer depends not only on contaminant physicochemical properties but also varies widely according to animal feeding and physiology^{5,6}. Aiming to go deeper into the understanding of the complex interplay between contaminant properties, lipid nutrition and animal physiology, an integrative and mechanistic approach should be developed. For such purpose, systemic modelling of the contaminant absorption, distribution, metabolism, and excretion (ADME) processes is the adequate media. Although fugacity-based⁷ or physiologically-based toxicokinetic (PBTK)⁸⁻¹⁰ models of lipophilic contaminant fate were previously developed for dairy cows, attempts in beef cattle are much scarcer. Bogdal *et al.*¹¹ introduced a PBTK model describing PCBs and PCDD/Fs fate in suckling calf, whereas MacLachlan and Buhla¹² described roughly weaned growing cattle with a generic one-compartment model. The aims were i) to set-up a mechanistic model describing the ADME of lipophilic contaminants in growing beef cattle and ii) to assess its suitability as a media to decipher the complex interplay between contaminant properties, lipid nutrition and animal physiology.

2 Materials and Methods

Rationale and overview. The fugacity-based PBTK model consists of three coupled models, one describing the lipophilic contaminant ADME, the second feed intake and lipid digestion, and the last cattle growth physiology (Figure 1). Such coupling was already implemented in lactating cows, offering a generic framework to explore the respective effects of contaminant physicochemical properties, lipid nutrition, and animal physiology on the feed-to-food toxicokinetic¹⁰.

ADME model. Mechanistic formalisms of lipophilic contaminant adjective, diffusive, and degradation flows are hybridized from previous dairy cow fugacity⁷ and PBTK⁹ models. The ADME is described within three digestive and six empty body compartments. Contaminant intake originates from the feed bunker, flows successively to the rumen and intestines, where it is excreted into feces or absorbed into blood. From blood, the contaminant is either excreted back to the intestines or distributed between liver, muscles, adipose tissues (first to blood-perfused, later to deep compartments), and rest of empty body. Metabolic clearance is represented in the liver. Advective flows (12 blue arrows, Figure 1) represent where the contaminant is transferred from one compartment to another together with an advective medium.

$$Adv. Flow Cont_{i \rightarrow j} (ng d^{-1}) = Q_{i \rightarrow j} (kg d^{-1}) \times A_i (ng) / M_i (kg) [/P_i (unitless)] \quad (1)$$

where $Q_{i \rightarrow j}$ is the rate of digesta transit or blood perfusion from i to j , A_i the contaminant amount in i and M_i the mass of i . The partition coefficient P_i reflects the tissue _{i} -blood ratio of the contaminant concentration at equilibrium and is only included for the flows from body tissue compartments back to blood.

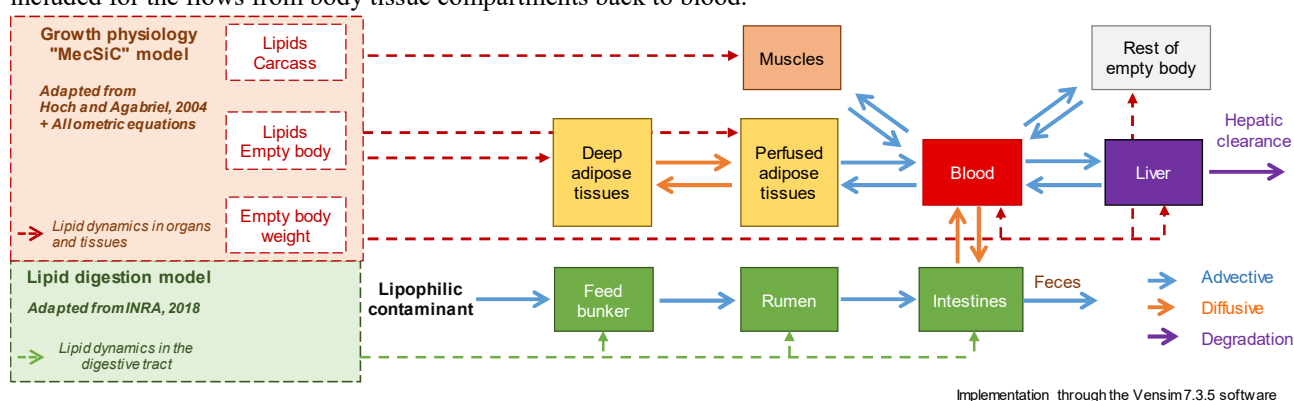


Figure 1. Conceptual diagram of the fugacity- and physiologically-based toxicokinetic (PBTK) model, describing the fate of a lipophilic contaminant into growing beef cattle.

The P_i is fixed to the tissue_i-blood ratio of total lipid concentrations⁸, assuming that non-polar lipophilic contaminants would diffuse almost exclusively into lipids.

Diffusive flows (four orange arrows, Figure 1) represent where the contaminant crosses the interface between two compartments by passive diffusion along the concentration gradient¹³. Two diffusive flows are represented at the intestines / blood interface for absorption and reverse non-biliary excretion. Indeed, non-polar lipophilic contaminants excreted from body to feces originate almost exclusively from such a passive diffusion process across the intestinal wall¹⁴. Two diffusive flows are implemented at the perfused / deep adipose tissues interface to represent the late (re)distribution pattern of lipophilic contaminants in adipose tissues^{7,15}. Perfused adipose represents the adipocytes' extra-cellular matrix, membrane and cytosol, whereas deep adipose figures the adipocytes' triglyceride-rich vacuoles. For both interfaces, the total diffusive transport includes the contaminant serial crossing of a water phase (unstirred water layer surrounding the microvilosity of the intestinal wall or adipocyte cytosol) and of a lipid phase (lipid bilayer of enterocyte or adipocyte membranes)^{7,13}. As diffusive transports occur in series, the sum of each single reciprocal value gives the total resistance to contaminant transport¹⁶.

$$\text{Diff. Flow Cont}_{i \rightarrow j} \text{ (ng d}^{-1}\text{)} = [A_i \text{ (ng)} / V_{\text{Lip}_i} \text{ (m}^3 \text{ lipids)}] / [(K_{ow} \text{ (unitless)} / Q_{\text{Wat}_i/j} \text{ (m}^3 \text{ d}^{-1}\text{)}) + (1 / Q_{\text{Lip}_i/j} \text{ (m}^3 \text{ d}^{-1}\text{)})] \quad (2)$$

where A_i is the contaminant amount in i , V_{Lip_i} the volume of lipids in i (lipid density of 820 kg m⁻³), K_{ow} the partition coefficient between octanol and water that converts a lipid- to a water-based concentration and $Q_{\text{Wat}_i/j}$ and $Q_{\text{Lip}_i/j}$ are the diffusive parameters across the water and lipid phases at the interface between i and j , respectively.

Liver is figured as the sole site for contaminant degradation (i.e., metabolism; purple arrow, Figure 1).

$$\text{Degr. Flow Cont}_{\text{liver}} \text{ (ng d}^{-1}\text{)} = k_{\text{met}} \text{ (d}^{-1}\text{)} \times A_{\text{liver}} \text{ (ng)} \quad (3)$$

where, k_{met} is the first-order metabolism rate constant and A_{liver} is the contaminant amount in liver. A linear reaction rate is assumed considering that in practical cases the range of diet and body contaminant concentrations are far from the ones that may induce or saturate the metabolism¹⁷.

The ADME model set-up requires the user to define 10 initial parameters: two regarding the contaminant properties (K_{ow} and k_{met}), the four tissue blood-perfusion rates reported by MacLachlan⁸, and the four diffusive parameters ($Q_{\text{Lip}_i/j}$ and $Q_{\text{Wat}_i/j}$) fitted according to the fugacity model of McLachlan⁷. The K_{ow} values are harvested from literature, whereas k_{met} should be fitted for every single contaminant against experimental data¹⁸. In order to further resolve the several equations of the ADME model, the time-dependent kinetics of body weight (BW), and of fresh and lipid masses in feed, digesta, feces and tissue compartments should be described. This is further accomplished thanks to the coupling with the lipid digestion and growth physiology models.

Lipid digestion and growth physiology models. The feed intake and lipid digestion model is based on the INRA feeding system¹⁹. Cattle intake capacity is first computed using the allometric Eqn. 19.18¹⁹, and corresponding coefficients depending on the sex and maturity of growing or finishing cattle (Table 19.3). Dry matter (DM) intake, and accordingly lipid and metabolized energy (ME) intakes are further derivated from the specific diet fill unit, and lipid and ME contents (e.g., harvested from chapters 25 and 26¹⁹). Lipid transit and absorption rate into the digestive tract are described according to Eqn. 3.32, 3.33, 4.1, 4.2 and 4.4¹⁹.

Body fresh and lipid mass kinetics are described by the teleonomic growth model “MecSiC”²⁰. The ME intake is the driving force and is allocated to either lipid or protein synthesis within the carcass and non-carcass compartments, depending on the genotype (sex and breed) and physiological age of the animal. Lipid and protein degradation depends on the state of the compartments. Net accretion or mobilization is further determined by the balance between synthesis and degradation for each of the four compartments. Parameter calibrations were performed against serial slaughter experiment databases for various types of growing cattle (e.g., Charolais bull or Angus steer²⁰). In the present study, a further development was achieved for the allocation of carcass and non-carcass lipid masses to the six specific body compartments represented in the ADME model (Figure 1). Accordingly, allometric equations estimating muscle and adipose tissue lipid masses from empty body lipid mass (available from “MecSiC”) were fitted using the slaughterhouse database of HerbiPole (<https://doi.org/10.15454/1.5572318050509348E12>).

Simulation setting. A set of contamination scenarios were simulated to assess the suitability of the fugacity-based PBTk model as a media to explore the interplay between contaminant properties, lipid nutrition and growth physiology. Accumulation kinetics of contaminants ranging from log K_{ow} 5 to 9 (typical range for PCDD/F and PCB congeners²¹) either unmetabolized ($k_{\text{met}} = 0 \text{ d}^{-1}$; e.g., 1,2,3,6,7,8-HxCDD) or moderately metabolized ($k_{\text{met}} = 5 \text{ d}^{-1}$; e.g., 1,2,3,7,8,9-HxCDF) were simulated in a two diets \times two cattle genotypes factorial design. One diet contained none (NoneLS; 29 g lipids kg⁻¹ DM), whereas the other 5% DM lipid supplementation (LS; 72 g lipids kg⁻¹ DM). Both contained 12 MJ ME kg⁻¹ DM and a contamination level of 0.57 ng TEQ kg⁻¹ DM (action level for PCDD/Fs, EU regulation 277/2012). The growth from 400 to 800 kg BW of an Angus \times Hereford steer (AH) or a “Blonde d’Aquitaine” bull (BA) were simulated. Net and apparent absorption rates, and the assimilation efficiency were further computed over the whole accumulation period.

$$\text{Net absorption (\%)} = \text{Diff. Flow Cont}_{\text{intestines} \rightarrow \text{blood}} / (\text{Diff. Flow Cont}_{\text{intestines} \rightarrow \text{blood}} + \text{Adv. Flow Cont}_{\text{intestines} \rightarrow \text{feces}}) \times 100 \quad (4)$$

$$\text{Apparent absorption (\%)} = (\text{Cont. Intake} - \text{Adv. Flow Cont}_{\text{intestines} \rightarrow \text{feces}}) / \text{Cont. Intake} \times 100 \quad (5)$$

$$\text{Assimilation efficiency (\%)} = \text{Final Cont. Body Burden (at 800 kg BW)} / \text{Cont. Intake} \times 100 \quad (6)$$

3 Results

Physiological traits. From 400 to 800 kg BW, the feed intake model suggested that the total DM intake, and accordingly contaminant dosing, was 1.5-fold higher in AH than in BA (in average 12.0 and 9.0 kg DM d⁻¹ over 359 and 317 days, respectively). Nonetheless, according to “MecSiC” simulations, the growth rate was still higher in BA than in AH (1.26 and 1.11 kg BW d⁻¹, respectively), with large differences in body composition characterized by lean BA (from 8.6% lipids in empty body at 400 kg BW to 10.7% at 800 kg) and fat-rich AH (20.2 to 35.9%). Body lipid accretion was therefore much faster in AH (0.53 kg lipids d⁻¹) than in BA (0.16 kg lipids d⁻¹). Also in AH, more body lipids were allocated to adipose tissues (from 55 to 81% of empty body total lipids) than in BA (43 to 57%).

Absorption rates and assimilation efficiencies. Mass balances of lipophilic contaminant fate along the whole simulation set-up are illustrated in Figure 2. Absorption rates were affected widely by the contaminant lipophilicity. For the NoneLS diet, absorption of around 80% of the contaminant intake were recorded for log K_{ow} lower than 6.5, whereas a sharp decrease occurred for log K_{ow} above 7.0, reaching only an absorption of 1–4% at log K_{ow} 9. Similar ranges of absorption rates were recorded whatever the metabolic susceptibility of the contaminant, which mainly affected the assimilation efficiency: up to 70% for unmetabolized ($k_{met} = 0$ d⁻¹) contaminants of K_{ow} lower than 6.5, compared to lower than 20% when k_{met} was set at 5 d⁻¹. Such effects of contaminant properties were consistent between diets, but LS diet resulted in lower maximal absorption rates of 50–60% and assimilation efficiencies of around 40% for unmetabolized and 10% for metabolized contaminants of log K_{ow} lower than 6.5. Additionally, LS diet led to 1.4-fold lower apparent (i.e., initially unabsorbed + endogenous excretion back from blood to intestines) than net absorption rates, compared to only 1.2-fold difference in NoneLS diet. Type of cattle slightly modulated further the absorption and assimilation, with for contaminants of moderate log K_{ow} (≤ 6.5) a slightly higher net absorption but lower assimilation in BA compared to AH (Figure 2).

Accumulation kinetics in muscles and adipose tissues. Simulations of contaminant concentrations in muscles and adipose tissues are illustrated in Figure 3. Model simulations suggested parallel kinetics in muscle and adipose tissue concentrations, with in the latter 1.1- and 4.0-fold lower concentrations for moderately (log $K_{ow} = 6$) and highly (log $K_{ow} = 8$) lipophilic contaminants, respectively. Unmetabolized and moderately lipophilic contaminant concentrations were up to 6-fold higher than the EU maximum regulatory limit, whereas levels reach only 3-fold the limit for unmetabolized and highly lipophilic, and never overpass it for metabolized ($k_{met} = 5$ d⁻¹) ones. Lipid supplementation decreased every contaminant concentrations at 800 kg BW from 1.7- to 3.0-fold for moderately and highly lipophilic contaminants, respectively. Besides, when compared to BA, AH had steadily lower adipose tissue concentrations in unmetabolized (3.0-fold lower at 800 kg BW) and in metabolized and highly lipophilic (2.5-fold lower) contaminants. In muscles, such effect was vanished for unmetabolized contaminants (1.7-fold lower in AH), and no more perceivable for metabolized ones.

4 Discussion

Contaminant physicochemical properties. When contaminant lipophilicity (i.e., log K_{ow}) increased, a curvilinear decrease in absorption rate and a higher difference between low adipose tissue and high muscle concentrations were reproduced by model simulations. The mechanistic view of the diffusive transfer into a water phase implies that when the contaminant K_{ow} increases, both the net absorption rate decreases and the time for distribution equilibrium to the deep adipose increases. This is well caught by simulations of the initial dairy cow fugacity model⁷, and by biological observations^{15,22–24}.

Lipid supplementation. Both a large decrease in net absorption rate and a higher excretion flow from blood back to intestines (i.e., net – apparent absorption rates) were deciphered in response to dietary lipid supplementation. Those effects are most presumably linked to increases in lipid mass within the intestines and lipid excretion through feces.

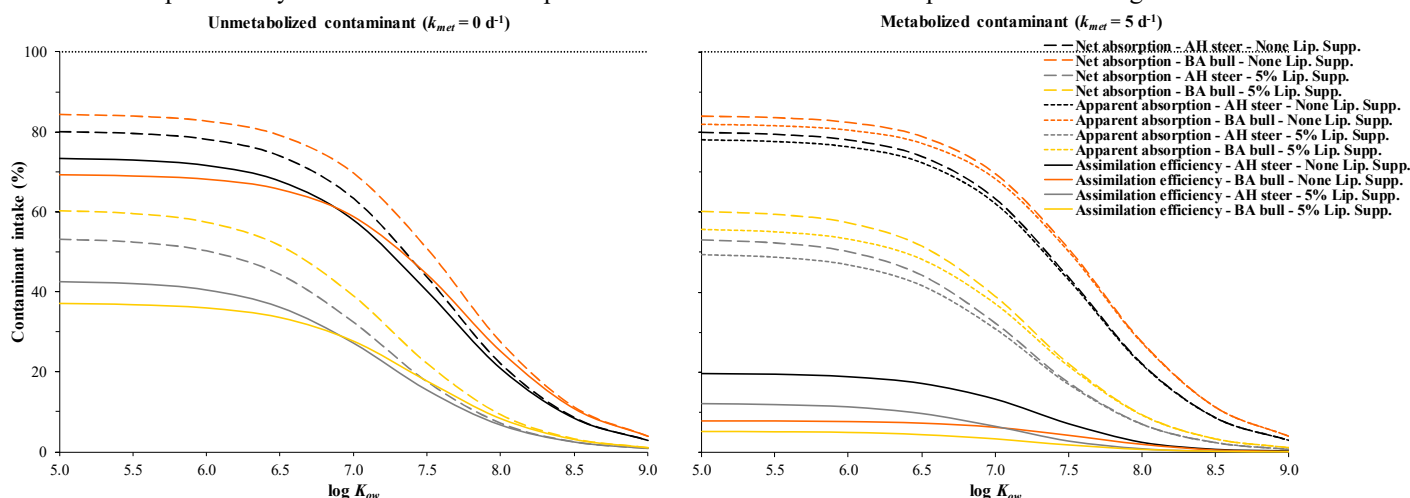


Figure 2. Net and apparent absorption rates and assimilation efficiencies of lipophilic contaminants depend on their lipophilicity (K_{ow}) and metabolic susceptibility (k_{met}) in Angus × Hereford (AH) steers or “Blonde d’Aquitaine” (BA) bulls, receiving none or 5% dietary lipid supplementation from 400 to 800 kg BW. For the unmetabolized contaminant (left panel), apparent absorption and assimilation efficiency are confounded.

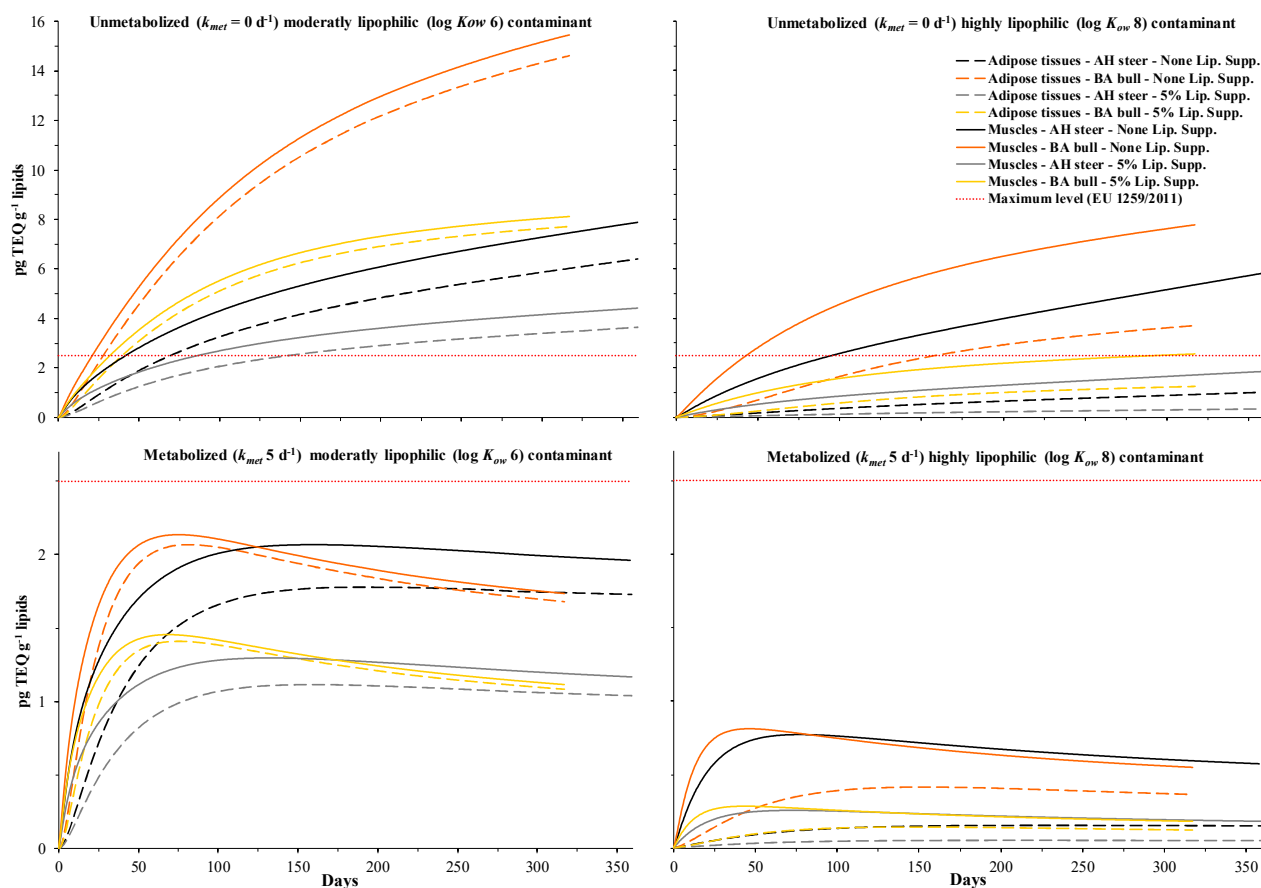


Figure 3. Accumulation kinetics of lipophilic contaminants in muscles and adipose tissues depend on lipophilicity (K_{ow}) and metabolic susceptibility (k_{met}) in Angus \times Hereford (AH) steers or “Blonde d’Aquitaine” (BA) bulls, receiving none or 5% dietary lipid supplementation from 400 to 800 kg BW.

Indeed, an increase in lipid content of digesta increases further their affinity for lipophilic contaminants, which limits the intestines to blood diffusive flow, and enhances the reverse blood to intestines diffusive and feces advective flows. Enhancement of fecal excretion of TCDD, PCBs and hexachlorobenzene due to digesta and feces lipid enrichments was experimentally outlined in sheep supplemented with non-absorbable lipids along a depuration phase^{24,25}.

Cattle physiology. Compared to AH, BA showed a slightly higher net absorption rate. This may be explained by a lower feed intake and accordingly lower intestine lipid mass (i.e., space of dilution for lipophilic contaminant) and fecal lipid excretion. Together, those would lead to a faster achievement of the intestines / blood diffusive equilibrium and decrease in contaminant fecal excretion, respectively. Conversely, a lower apparent absorption rate was recorded in BA for unmetabolized contaminants. A higher rate of the diffusive flow back from blood to intestines (i.e., net – apparent absorption rates) would explain such discrepancy, and is presumably linked to the higher contaminant concentration in blood of BA compared to AH. Indeed, even if AH showed higher assimilation rates in unmetabolized contaminants, contamination levels in body tissues were still lower than in BA. The basis of this discrepancy relies mainly on a dilution effect in fat-rich AH, as if their body contaminant burden was until 1.6-fold higher, body lipid mass was concomitantly 3.6-fold over the ones of the lean BA. Such a dilution effect due to increase in fatness was previously highlighted experimentally for PCB bioconcentration and biotransfer factors in beef bulls⁶.

5 Conclusions

The growing cattle fugacity-based PBTK model fulfilled the aim of deciphering the complex interplay between contaminant, diet and animal physiology on the ADME of lipophilic contaminants. Ongoing developments include the calibration of the hepatic metabolism rate for a wide range of lipophilic contaminants, and assessment of the model predictive capabilities. Those steps will allow the delivery of an integrative tool for risk assessors and managers, and ultimately contribute to the chemical safety towards regulated and emerging contamination risks of diverse beef meat production systems.

6 Acknowledgments

This communication is dedicated in memory of Prof. Daniel Sauvant who was largely involved in the model development. The authors would like to warmly thank Jacques Agabriel (INRAE UMRH, Saint-Genès-Champagnelle, France) for insightful advices, contribution, and support along the project.

7 References

1. Hoogenboom R, Traag W, Fernandes A, Rose M (2015) European developments following incidents with dioxins and PCBs in the food and feed chain. *Food Control*. 50:670-683.
2. Zennegg M (2018) Dioxins and PCBs in Meat – Still a Matter of Concern? *Chimia*. 72:690-696.
3. BAG (2012) Dioxine und PCB in Rindfleisch aus naturnaher Produktion. pp 1-4.
4. BVL (2013) Berichte zur Lebensmittelsicherheit. Bundesweiter Überwachungsplan 2011. Gemeinsamer Bericht des Bundes und der Länder. pp 1-71.
5. Driesen C, Lerch S, Siegenthaler R, Silacci P, Hess HD, Nowack B, Zennegg M (2022) Accumulation and decontamination kinetics of PCBs and PCDD/Fs from grass silage and soil in a transgenerational cow-calf setting. *Chemosphere*. 296:133951.
6. Driesen C, Zennegg M, Morel I, Hess HD, Nowack B, Lerch S (2021) Average transfer factors are not enough: The influence of growing cattle physiology on the transfer rate of polychlorinated biphenyls from feed to adipose. *Chemosphere*. 270:129698.
7. McLachlan MS (1994) Model of the fate of hydrophobic contaminants in cows. *Environ. Sci. Technol.* 28:2407-2414.
8. MacLachlan DJ (2009) Influence of physiological status on residues of lipophilic xenobiotics in livestock. *Food Addit. Contam. Part A-Chem.* 26:692-712.
9. Derks HJGM, Berende PLM, Olling M, Everts H, Liem AKD, De Jong APJM (1994) Pharmacokinetic modeling of polychlorinated dibenzo-p-dioxins (PCDDs) and furans (PCDFs) in cows. *Chemosphere*. 28:711-715.
10. Lerch S, Martin O, Fournier A, Henri J (2018) Exploring the effects of dietary lipid content and digestibility on lipophilic contaminants transfer from feed to milk in dairy cows: insights from a physiologically-based toxicokinetic modelling approach. *Adv. Anim. Biosci.* 9:444.
11. Bogdal C, Züst S, Schmid P, Gyalpo T, Zeberli A, Hungerbühler K, Zennegg M (2017) Dynamic transgenerational fate of polychlorinated biphenyls and dioxins/furans in lactating cows and their offspring. *Environ. Sci. Technol.* 51:10536-10545.
12. MacLachlan DJ, Bhula R (2009) Transfer of lipid-soluble pesticides from contaminated feed to livestock, and residue management. *Anim. Feed Sci. Technol.* 149:307-321.
13. Kelly BC, Gobas FA, McLachlan MS (2004) Intestinal absorption and biomagnification of organic contaminants in fish, wildlife, and humans. *Environ. Toxicol. Chem.* 23:2324-2336.
14. Jandacek RJ, Tso P (2001) Factors affecting the storage and excretion of toxic lipophilic xenobiotics. *Lipids*. 36:1289-1305.
15. Richter W, McLachlan MS (2001) Uptake and transfer of PCDD/Fs by cattle fed naturally contaminated feedstuffs and feed contaminated as a result of sewage sludge application. 2. Nonlactating cows. *J. Agric. Food Chem.* 49:5857-5865.
16. Mackay D (2001) Multimedia environmental models: the fugacity approach. CRC Press Taylor & Francis Group: Ann Arbor, 2001; 2nd edition, pp. 272.
17. Cahill TM, Cousins I, Mackay D (2003) Development and application of a generalized physiologically based pharmacokinetic model for multiple environmental contaminants. *Environ. Toxicol. Chem.* 22:26-34.
18. Feil VJ, Huwe JK, Zaylskie RG, Davison KL, Anderson VL, Marchello M, Tiernan TO (2000) Chlorinated dibenzo-p-dioxin and dibenzofuran concentrations in beef animals from a feeding study. *J. Agric. Food Chem.* 48:6163-6173.
19. INRA (2018) INRA feeding system for ruminants. Wageningen Academic Publishers. pp. 640.
20. Hoch T, Agabriel J (2004) A mechanistic dynamic model to estimate beef cattle growth and body composition: 1. Model description. *Agric. Syst.* 81:1-15.
21. Amutova F, Delannoy M, Baubekova A, Konuspayeva G, Jurjanz S (2021) Transfer of persistent organic pollutants in food of animal origin – Meta-analysis of published data. *Chemosphere*. 262:128351.
22. Driesen C, Zennegg M, Myriam R, Sébastien D, Ueli W, Nowack B, Lerch S (2022) Transgenerational mass balance and tissue distribution of PCBs and PCDD/Fs from grass silage and soil into cow-calf continuum. *Chemosphere*. 307:135745.
23. Driesen C, Zennegg M, Siegenthaler R, Lerch S (2022) Transgenerational absorption, distribution, metabolism, and excretion of PCBs in beef cows and calves. *Organohalogen Compd.* 84.
24. Rey-Cadilhac L, Cariou R, Ferlay A, Jondreville C, Delavaud C, Faulconnier Y, Alcouffe S, Faure P, Marchand P, Le Bizec B, Jurjanz S, Lerch S (2020) Undernutrition combined with dietary mineral oil hastens depuration of stored dioxin and polychlorinated biphenyls in ewes. 1. Kinetics in blood, adipose tissue and faeces. *PlosOne*. 15:e0230629.
25. Rozman K, Rozman T, Greim H, Nieman IJ, Smith GS (1982) Use of aliphatic-hydrocarbons in feed to decrease body burdens of lipophilic toxicants in livestock. *J. Agric. Food Chem.* 30:98-100.